

Combining interpolation and 3D level set method (I+3DLSTM) for medical image segmentation

T. Doshi, G. Di Caterina, J. Soraghan, L. Petropoulakis, D. Grose, K. MacKenzie and C. Wilson

A combined interpolation - 3D Level Set Method (I+3DLSTM) based segmentation process is presented. The performance in terms of accuracy of the 3-dimensional (3D) level set method (LSM) in the segmentation of throat regions from highly anisotropic magnetic resonance imaging (MRI) volumes, with and without an interpolation step is evaluated. Qualitative and quantitative results from real MRI data suggest that performing interpolation, to reconstruct isotropic MRI volumes, prior to 3D LSM improves the accuracy of the segmentation results, compared to interpolation post 3D LSM and no interpolation at all.

Introduction: 3-dimensional (3D) level set method (LSM) [1-2] is widely used for the segmentation of anatomical structures from medical imaging volumes with promising results [3-5]. In 3D LSM, a closed 3D surface $S(t)$ propagates in time towards the desired boundaries through the iterative evolution of a 4D implicit function known as level set function $\phi(X, t)$. The surface $S(t)$ is embedded as a zero level set of the implicit function ϕ , $S(t) = \{X \in R^3 / \phi(X, t) = 0\}$ and ϕ is evolved according to:

$$\frac{\partial \phi}{\partial t} + F|\nabla \phi| = 0 \quad (1)$$

where F is a scalar velocity function typically driven by external volume-dependent terms, which drive ϕ to the desired object boundaries, and internal geometric terms such as mean curvature motion, which keep ϕ smooth. This implicit representation of 3D surface allows change of topology and is useful for the shape recovery of complex anatomical structures. Another desirable feature of LSM is that numerical computations can be performed on a fixed Cartesian grid, where elements are unit cubes, without having to parameterize the points on a surface as in parametric active contour models [2]. Therefore, to be able to apply 3D LSM to anisotropic (non-cubic) medical imaging volumes, where the distance between consecutive slices along the z-dimension is significantly greater than the in-plane (x-y) pixel size (Fig. 1a), interpolation is performed in [3-5] to reconstruct isotropic (cubic) volumes before segmentation using 3D LSM. However, no direct numerical comparison is provided in [3-5] between segmentation results obtained from 3D LSM only and segmentation results obtained from interpolation before and after 3D LSM, to validate the importance of performing interpolation before 3D LSM. This Letter demonstrates the significance of applying interpolation before 3D LSM for the segmentation of throat regions, with variable topology (Fig. 1b), from anisotropic medical imaging volumes. The novelty of this work lies in a generalised approach where interpolation and 3D LSM does not require any statistical or morphological information of the region of interest. Qualitative and quantitative results show that interpolation before 3D LSM, to produce isotropic volume, further improves the segmentation accuracy of the 3D LSM, by allowing it to successfully segment the concave boundaries and multiple regions of the throat when throat region is split into two or more regions on the same MRI slice.

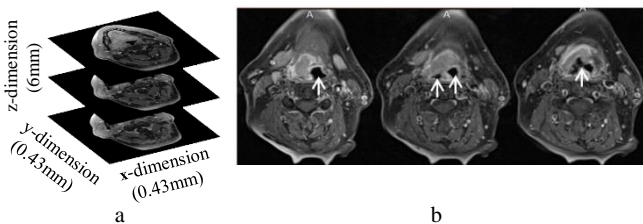


Fig. 1 Axial slices from MRI volume

a Demonstrating anisotropic voxel size in x-, y-, and z-dimensions
b Demonstrating change in topology (splitting and merging) of the throat region (as highlighted by the white arrows)

Method: For the segmentation of the throat regions, contrast-enhanced T1-weighted MRI scans were obtained for 12 patients using typical clinical imaging parameters from 1.5T MRI scanners, with range of $0.43 \times 0.43 - 0.94 \times 0.94 \text{mm}^2$ in-plane (x-y) resolution, 3-5mm slice thickness and 3.3-6mm spacing in between slices. The number of axial slices in each MRI scans ranged from 7 to 17. All real axial MRI slices were pre-processed to remove background noise and intensity inhomogeneity [5]. Fourier based inter-slice interpolation [6] was performed along z-dimension (Fig. 1a), to add axial interpolated slices in between pre-processed real MRI slices, to produce isotropic voxel size (same size in z-dimension as in x- and y-dimensions) and to reduce uncertainties between slices. The Fourier approach was chosen as interpolation technique due to its simplicity and accuracy compared to other spatial interpolation methods [7]. The number of axial slices in the MRI scans after interpolation ranged from 43 to 155. MRI volumes were reconstructed using real and interpolated slices and throat region was segmented from reconstructed isotropic volumes using 3D LSM [5]. The speed function F used in 3D LSM for the segmentation depends on the intensity (grey scale) value of input data I at the point (x, y, z) and is given as:

$$F = \alpha(\varepsilon - |I(x, y, z) - T|) + (1 - \alpha) \nabla \cdot \frac{\nabla \phi}{|\nabla \phi|} \quad (2)$$

where $\nabla \cdot \frac{\nabla \phi}{|\nabla \phi|}$ is the mean curvature of the surface, T is the mean and

ε is the variance of the region to be segmented and $\alpha \in [0, 1]$ is a free parameter which controls the weighting between two terms. Further details on the level set function and related parameters used can be found in [5].

Results and discussion: To demonstrate the significance of interpolation before 3D LSM to accurately segment throat regions from anisotropic volumes, comparisons between Matlab implementations of 3D LSM with and without interpolation on 12 MRI volumes are reported in this section. For comparison, the technique of using interpolation prior to 3D LSM is referred as 'I+3DLSTM', technique of using only 3D LSM is referred as '3DLSTM' and technique of using interpolation after 3D LSM is referred as '3DLSTM+I'.

For quantitative comparison, manual segmentation of the throat regions was obtained from a medical expert using real MRI slices. These are used as reference segmentation. The F-measure [5] which estimates the algorithmic accuracy by considering true positive, true negative, false positive and false negative pixels was calculated on slice-by-slice basis between reference and I+3DLSTM segmentation results denoted as $F\text{-measure}_{I+3DLSTM}$, and between reference and 3DLSTM segmentation results denoted as $F\text{-measure}_{3DLSTM}$. The F-measure values for 3D LSM+I are similar to $F\text{-measure}_{3DLSTM}$ on real MRI slices. This is because in 3DLSTM+I, the interpolation is carried out to add outlines in between the segmentation outlines obtained from real MRI slices. Thus, there is no change in the segmentation outlines on real MRI slices.

The F-measure values range from 0 to 1, with 1 value means perfect agreement with reference segmentation. The change in accuracy ($\nabla \text{accuracy}$) between $F\text{-measure}_{I+3DLSTM}$ and $F\text{-measure}_{3DLSTM}$ was calculated in percentage (%) as:

$$\nabla \text{accuracy} (\%) = \frac{F\text{-measure}_{I+3DLSTM} - F\text{-measure}_{3DLSTM}}{F\text{-measure}_{3DLSTM}} \times 100 \quad (3)$$

Fig. 2 shows segmented throat region (yellow outline) on an MRI slice, with the lowest F-measure value (0.3142), obtained using 3DLSTM (Fig. 2a) and the corresponding segmented throat regions (yellow outlines) from I+3DLSTM (F-measure: 0.6185) (Fig. 2b). The outline obtained by 3DLSTM+I is similar to the outline obtained by 3DLSTM. Thus, 3DLSTM+I outline is not included in Fig. 2. Visually comparing the results, it can be observed that I+3DLSTM was able to segment both regions of the throat (yellow outlines Fig. 2b) whereas the 3DLSTM segmented only one part of the throat region (yellow outline Fig. 2a).

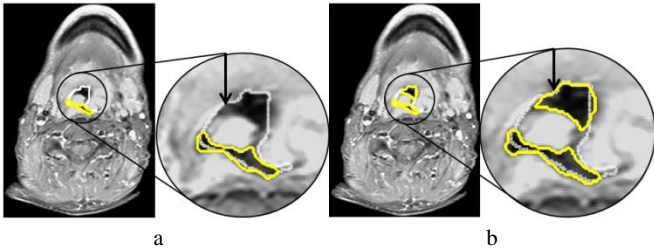


Fig. 2 Illustration of segmented throat region (yellow outline) using
a 3DLSM
b 3DLSM+I

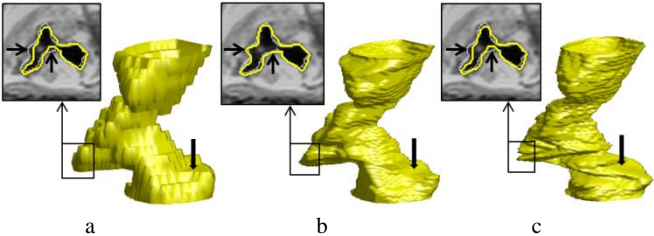


Fig. 3 Illustration of throat volume (yellow outline) obtained using
a 3DLSM
b I+3DLSM
c 3DLSM+I

This missing region (black arrow in Fig. 2a) can be attributed to the large spacing (6mm) in between real MRI slices. The throat region in the previous slice to the slice in Fig. 2a and missing region in Fig. 2a are not connected components. This non-connectivity contributes to the collapsing of the level set function and missing the region in the slice in Fig. 2a and in subsequent slices. However, due to interpolation, the smooth variation in the throat region in I+3DLSM allowed segmentation of both regions which is comparable to the reference segmentation (white* outline) and increased accuracy for that particular slice by 81.84%.

Fig. 3 shows segmented throat volumes obtained using 3DLSM (Fig. 3a), I+3DLSM (Fig. 3b) and 3DLSM+I (Fig. 3c). It can be seen that all three volumes appear visually similar; however, I+3DLSM eliminates the need for further smoothing of the throat volume and remove staircase effect observed (indicated by black open arrow in Fig. 3) in throat volumes segmented by 3DLSM and 3DLSM+I. Further, Fig. 3 also illustrates the performance accuracy in the segmented region (black box) using I+3DLSM, particularly in the concave regions (black arrows on 2D slice) as interpolation step extend the capture range of the 3DLSM and provide good convergence to boundary concavities. Thus, interpolation step before 3DLSM increased overall accuracy by 2.78% for this particular dataset with 6.86% increase for the slice shown in Fig. 3 compared to 3DLSM and 3DLSM+I.

The quantitative (F-measure) values for 3DLSM, I+3DLSM and 3DLSM+I in Fig. 4 shows increase in F-measure values and thus, increase in accuracy, with the range from minimum of 0.27% to maximum of 14.86% and average of 4.80%, for all 12 MRI volumes due to interpolation before 3DLSM. It was observed that the maximum increase in accuracy (14.86%) for I+3DLSM was observed for the dataset with maximum slice spacing (6mm) and minimum increase (0.27%) for minimum slice spacing (3.3mm). Further, low F-measure values for 3DLSM and 3DLSM+I compared to the reference segmentation is due to the large number of false negative pixels (e.g.: 353 pixels for particular slice) as uncertainties in between slices underestimate the throat area. The interpolation step before LSM segmentation reduced these uncertainties thus; reducing false negative pixels (to 76 pixels). The limitation of I+3DLSM, however, is that in some MRI slices it slightly overestimate (maximum false positive pixels: 59) the throat area when compared to reference segmentation, particularly on the slices where the throat region is small. From a clinical view point this overestimation, however, is preferable to an underestimation due to the dangers of recurrence of disease from undertreating the target. Overall, quantitative results agree with visual

results that I+3DLSM segmentation results provide comparable result to the reference segmentation compared to 3DLSM and 3DLSM+I.

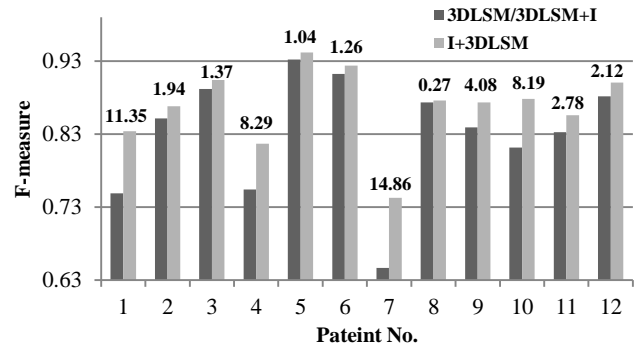


Fig. 4 F-measure values for 3DLSM, I+3DLSM and 3DLSM+I with Accuracy(%) values (data labels on each patient)

Conclusion: This Letter compared the 3D LSM segmentation results of the throat regions from anisotropic MRI volumes with and without interpolation step. Experimental results show that an interpolation before 3D LSM (I+3DLSM) technique produce more accurate results compared to 3DLSM and an interpolation after 3DLSM (3DLSM+I). This was particularly observed in the presence of change of topology and concave regions of the throat region.

Acknowledgments: The authors would like to acknowledge the Beatson Cancer Charity for their financial support with this study.

T. Doshi*, G. Di Caterina, J. Soraghan and L. Petropoulakis (*CeSIP, Department of Electronic and Electrical Engineering, University of Strathclyde, 204 George Street, Glasgow, G1 1XW, United Kingdom*)

E-mail: trushali.doshi@strath.ac.uk

D. Grose and C. Wilson (*Beatson West of Scotland Cancer Centre, Gartnavel Hospital, Glasgow G12 0YN*)

K. MacKenzie (*Glasgow Royal Infirmary, Glasgow, G4 0SF*)

References

1. S. Osher, R.Fedkiw. 'Level Set Methods and Dynamic Implicit Surfaces', (Springer-Verlag, 2003).
2. D. Mageea, A. Bulpitt and E. Berry, 'Level Set Methods for the 3D Segmentation of CT Images of Abdominal Aortic Aneurysms', *Med. Image Understand. Anal.*, 2001, pp. 141-144.
3. S. Soleimanifard, M. Schar, A. Hays, et al, 'Vessel Centerline Tracking and Boundary Segmentation in Coronary MRA with Minimal Manual Interaction', *Int. Symp. Biomed Imaging*, 2012, pp. 1417-1420
4. A. Yushkevich, J. Piven, H. Hazlett, et al. 'User-guided 3D active contour segmentation of anatomical structures: Significantly improved efficiency and reliability'. *Neuroimage*, 2006, vol. 31, no. 3, pp. 1116-1128.
5. S. Campbell, T. Doshi, J. Soraghan et al., '3-dimensional throat region segmentation from MRI data based on Fourier interpolation and 3-dimensional level set methods', *IEEE Eng. Med Biol. Soc.*, 2015, pp. 2419-2422.
6. J. Adams, 'A subsequence approach to interpolation using the FFT', *IEEE Trans Circuits and Systems*, 1987, vol. 34, no. 5, pp. 568 - 570.
7. W. Hawkins, 'FFT interpolation for arbitrary factors: a comparison to cubic spline interpolation and linear interpolation', *Nuclear Sci. Sys. Med. Imag.*, 1994, vol.3, pp. 1433 - 1437.